

A novel discrete variable representation for quantum mechanical reactive scattering via the Smatrix Kohn method

Daniel T. Colbert and William H. Miller

Citation: *The Journal of Chemical Physics* **96**, 1982 (1992); doi: 10.1063/1.462100

View online: <http://dx.doi.org/10.1063/1.462100>

View Table of Contents: <http://scitation.aip.org/content/aip/journal/jcp/96/3?ver=pdfcov>

Published by the [AIP Publishing](#)

Articles you may be interested in

[Combining the discrete variable representation with the Smatrix Kohn method for quantum reactive scattering](#)

J. Chem. Phys. **99**, 9681 (1993); 10.1063/1.465450

[A collocation approach for quantum scattering based on the Smatrix version of the Kohn variational principle](#)

J. Chem. Phys. **91**, 7537 (1989); 10.1063/1.457277

[Quantum reactive scattering via the Smatrix version of the Kohn variational principle: Differential and integral cross sections for D+H₂ HD+H](#)

J. Chem. Phys. **91**, 1528 (1989); 10.1063/1.457650

[Comment on: "Quantum scattering via the Smatrix version of the Kohn variational principle"](#)

J. Chem. Phys. **89**, 4454 (1988); 10.1063/1.454784

[Quantum scattering via the Smatrix version of the Kohn variational principle](#)

J. Chem. Phys. **88**, 6233 (1988); 10.1063/1.454462



Re-register for Table of Content Alerts

Create a profile.



Sign up today!



similar applications of the related collocation method, and Friesner and colleagues¹⁴ have developed and utilized similar methods for the electronic Schrödinger equation. The DVR is a grid-point representation and it solves the problem of integral evaluation because there are no integrals to evaluate. It also helps solve the linear algebra problem because the Hamiltonian matrix is extremely *sparse*—the matrix of the potential energy is diagonal and that of the kinetic energy is a sum of one-dimensional matrices—which means that Lanczos-type (iterative) linear algebra methods^{2(c),15} can deal efficiently with extremely large systems. More on this in Sec. II.

Peet *et al.*¹⁶ have shown previously that DVR and collocation methods can in principle be used efficiently in S -matrix Kohn variational calculations, but this previous work was not readily generalizable to *reactive* scattering. The primary purpose of the present paper is thus to present a DVR methodology that does deal with *reactive scattering* and efficiently so. The specific DVR we have devised also has a particularly simple and generic or universal character; it involves only the grid points themselves, with no explicit reference to an underlying basis set, both for the construction of the Hamiltonian matrix and its subsequent use in the Kohn scattering calculation. We believe that this particular DVR and the adaptive nature of the energy cut-off scheme discussed below [in relation to Eq. (2.8)] should also be of use for quantum eigenvalue calculations.

Section II first describes the particular DVR scheme that we use; it is not only extremely simple, but quite an efficient basis. It is then shown in Sec. III how this DVR is utilized in the S -matrix Kohn method for reactive scattering and numerical examples to illustrate it are presented in Sec. IV. For the benchmark $H + H_2 \rightarrow H_2 + H$ reaction, e.g., it is seen that the number of DVR grid points needed to achieve a given degree of convergence is approximately the same as the number of conventional basis functions used in previous S -matrix Kohn calculations.

II. DISCRETE VARIABLE REPRESENTATION (DVR) WITH A UNIFORM GRID/FOURIER BASIS

We seek as *generic* and universal a DVR scheme as possible in order to be able to apply it as a “black box” procedure for complex problems. To this end, our thinking has been influenced by the many applications of “wave packet propagation on a grid” by Fourier transform methods, stimulated primarily by the work of Kosloff and co-workers.¹⁷ This has led us to choose a uniform (i.e., equally spaced) grid in the coordinates, for which the corresponding basis set is a Fourier basis. All the DVR transformations¹¹ can be carried out completely analytically in this case and the novel aspect of our approach is that we then take the infinite order limit. Appendix A carries out this calculation and here we summarize the results. A particularly appealing feature is that the DVR kinetic energy matrix so obtained is not only extremely simple, but also universal, i.e., independent of the specific basis used to derive it.

We first discuss this for the case of one dimension and show some illustrative examples and then show how it generalizes for multidimensions and non-Cartesian coordinates.

A. One Cartesian dimension

For one Cartesian dimension, $-\infty < x < \infty$, Appendix A shows that the DVR, i.e., grid point representation of the kinetic energy is [cf. Eq. (A7)]

$$T_{ii'} = \frac{\hbar^2 (-1)^{i-i'}}{2m\Delta x^2} \begin{cases} \pi^2/3, & i = i' \\ \frac{2}{(i-i')^2}, & i \neq i' \end{cases}, \quad (2.1)$$

the only parameter involved being the grid spacing Δx , or the “energy quantum of the grid” $\hbar^2/(2m\Delta x^2)$. The potential energy is, as usual,¹¹ diagonal

$$V_{ii'} = \delta_{ii'} V(x_i) \quad (2.2a)$$

and the grid points $\{x_i\}$ are uniformly spaced

$$x_i = i\Delta x, \quad i = 0, \pm 1, \pm 2, \dots \quad (2.2b)$$

One can also view Eq. (2.1) as an infinite order finite difference approximation for the second derivative; see Appendix B. Recall, e.g., the simple three-point finite difference approximation for a second derivative

$$f''(x_0) \cong -\frac{1}{\Delta x^2} [2f(x_0) - f(x_1) - f(x_{-1})], \quad (2.3a)$$

or more generally the $(2N+1)$ -order expression

$$f''(x_0) = -\frac{1}{\Delta x^2} \sum_{n=-N}^N A_n f(x_n); \quad (2.3b)$$

the three-point and five-point approximations, e.g., have $A_0 = 2$, $A_{\pm 1} = -1$, and $A_0 = 5/2$, $A_{\pm 1} = -4/3$, $A_{\pm 2} = 1/12$, respectively. Appendix B shows that the infinite order finite difference result is the same as that implied by Eq. (2.1), i.e., $A_0 = \pi^2/3$, $A_{\pm n} = 2(-1)^n/n^2$, for $n = 1, 2, \dots$. Table I lists these coefficients $\{A_n\}$ for several low order finite difference cases, compared to the infinite order result, to show how the $N \rightarrow \infty$ limit is approached. The grid representation of the kinetic energy in Eq. (2.1) is thus a property of the grid itself and not tied to any specific underlying basis set.

TABLE I. Coefficients $\{A_n\}$ of Eq. (2.3b) for the finite difference approximation to a second derivative. $2N+1$ is the number of points and $A_{-n} = A_n$.

$2N+1$	3	5	7	∞
0	2.000	2.500	2.722	3.290
1	-1.000	-1.333	-1.667	-2.000
2	0	0.083	0.150	0.500
3		0	-0.011	-0.222
4			0	0.125
5				-0.080
6				0.056
7				-0.041
8				0.031
9				-0.025
10				0.020

B. Simple test

It is useful to have some indication of how many grid points are necessary for this DVR to provide an accurate description a quantum system. This will be explored for reactive scattering in Sec. IV, but it is perhaps helpful here to test it on a simple one-dimensional eigenvalue problem, the harmonic oscillator. (We have carried out similar calculations for the Morse potential and the conclusions are essentially identical.) In units with $\hbar = m = \omega = 1$, the DVR Hamiltonian matrix is thus

$$H_{ii'} = \frac{(-1)^{(i-i')}}{2\Delta x^2} \left\{ \begin{array}{ll} \pi^2/3, & i = i' \\ \frac{2}{(i-i')^2}, & i \neq i' \end{array} \right\} + \delta_{ii'} \frac{x_i^2}{2}. \quad (2.4)$$

One potential concern about the infinite order DVR kinetic energy matrix [Eq. (2.1)] is that it does indeed correspond to an infinite grid and the decay of the matrix elements away from the diagonal is relatively slow, $(i-i')^{-2}$. Any real calculation must of course be made with finite matrices, i.e., a finite number of grid points. Our strategy is to use the infinite order expression (2.1), but simply to delete grid points, where the wave function is negligibly small, e.g., in energetically inaccessible regions. This forces the wave function to vanish at points not included in the grid and thus corresponds to placing the wave function in a box whose dimensions are determined by the grid points retained. A simple way to accomplish this is to introduce an energy cut-off V_c for the potential energy and to discard grid points $\{x_i\}$ for which

$$V(x_i) > V_c, \quad (2.5)$$

i.e., where the wave function for states with energies sufficiently below V_c will be negligibly small. Light *et al.*^{9(a),11} have used this idea previously in a variety of truncation and contraction methods employing DVRs. Convergence of the calculation can be checked by increasing the energy cutoff.

The correct eigenvalues for the present harmonic oscillator example are $E_n = n + 1/2$. Figures 1 and 2 show the fractional error $(E_{\text{approximate}}/E_{\text{exact}} - 1)$ that results from diagonalizing the DVR Hamiltonian [Eq. (2.4)] for various quantum states n as a function of the grid spacing Δx (Fig. 1) and the cut-off energy V_c (Fig. 2). Figure 1 shows that a smaller grid spacing is necessary to achieve a given level of accuracy the higher the quantum state; this is expected because higher states have shorter de Broglie wavelengths. The number of grid points per de Broglie wavelength, however, is approximately the same for all states; e.g., \sim three to four grid points per de Broglie wavelength achieves a relative accuracy of $\sim 10^{-4}$ – 10^{-5} . Figure 2 shows that a higher energy cutoff is required to achieve a given level of accuracy the higher the state, also an expected result. To achieve 10^{-3} relative accuracy (i.e., 0.1%), e.g., requires an energy cutoff approximately 2.5 (in units of $\hbar\omega$) above the energy level of interest.

Since the total interval spanned with an energy cutoff V_c is $2\sqrt{2V_c}$, the total number of grid points N for given values of Δx and V_c is

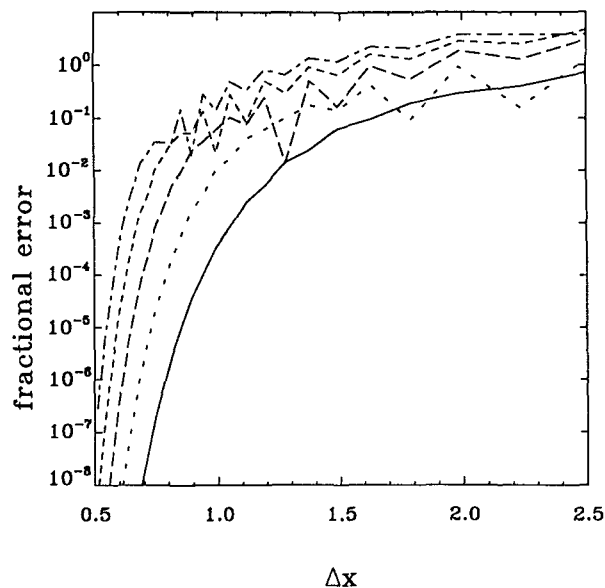


FIG. 1. The fractional error $(E_{\text{DVR}}/E_{\text{exact}} - 1)$ given by diagonalizing the DVR Hamiltonian for the harmonic oscillator [Eq. (2.4)] as a function of the grid spacing Δx . The lowest curve is for the state $n = 0$ and the successive higher ones are for states $n = 2, 4, 6, 8$. (Odd states fall in between the even ones and are omitted for clarity.)

$$N = 2\sqrt{2V_c}/\Delta x.$$

From Figs. 1 and 2, one can then deduce that the total number of grid points needed to achieve 0.1% relative accuracy (10^{-3}), e.g., is $N = 5, 10,$ and 15 for quantum states $n = 0, 4,$ and 8 , respectively.

C. Multidimensional generalization

The multidimensional generalization of a DVR is straightforward.¹¹ For three Cartesian degrees of freedom

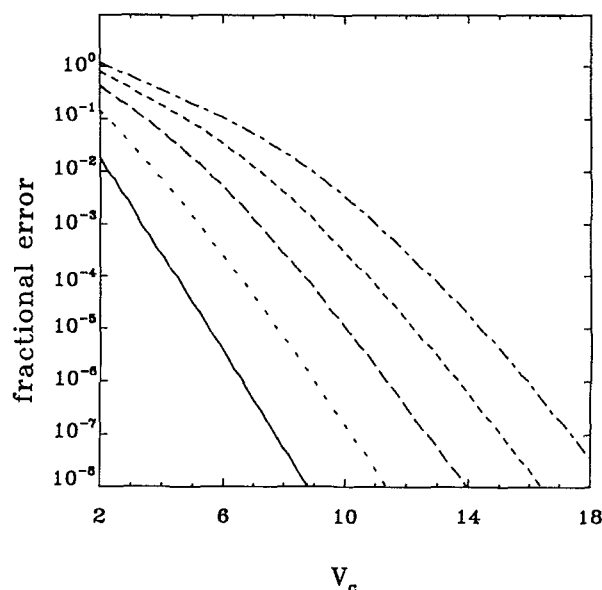


FIG. 2. The fractional error for the DVR harmonic oscillator, as in Fig. 1, as a function of the energy cut-off parameter V_c . The lowest curve is for state $n = 0$ and successive higher ones for $n = 2, 4, 6, 8$.

(x, y, z) , e.g., the Hamiltonian matrix is

$$H_{ijk, i'j'k'} = T_{ii'} \delta_{jj'} \delta_{kk'} + T_{jj'} \delta_{ii'} \delta_{kk'} + T_{kk'} \delta_{ii'} \delta_{jj'} + \delta_{ii'} \delta_{jj'} \delta_{kk'} V(x_i, y_j, z_k), \quad (2.6)$$

where for the present DVR, the three one-dimensional kinetic energy matrices are all of the form of Eq. (2.1). If the masses m_x , m_y , and m_z are different for the three degrees of freedom, one chooses the three grid spacings in a mass-weighted fashion, i.e., so that $m_x \Delta x^2 = m_y \Delta y^2 = m_z \Delta z^2$.

Not only is this Hamiltonian matrix extremely simple to construct (i.e., no integrals are involved and there is no reference to any specific underlying DVR basis functions), but the linear algebra problem is greatly simplified because the \mathbf{H} matrix is so sparse, as it is for all DVRs.¹¹ All of the iterative, Lanczos-type methods^{2(c),15} for large linear algebra calculations have as their rate limiting step the multiplication of the Hamiltonian matrix \mathbf{H} into a vector $\mathbf{H}\mathbf{v}$, which is in general an N^2 operation where N is the dimension of the \mathbf{H} matrix. For the case of f degrees of freedom [e.g., $f = 3$ in Eq. (2.6)], one has $N = n^f$, where n is the number of grid points per degree of freedom. Because of the simple structure of the Hamiltonian matrix of Eq. (2.6), however, one sees that the calculation of $\mathbf{H}\mathbf{v}$ requires many fewer operations (i.e., multiplications) than $N^2 = n^{2f}$ —multiplication of the potential energy matrix \mathbf{V} into a vector \mathbf{v} requires only $N = n^f$ multiplications (because \mathbf{V} is diagonal) and it is not hard to conclude that multiplication by the kinetic energy matrix requires $f \cdot n \cdot N = fn^{f+1}$ multiplications. Multiplication by the kinetic energy matrix is thus the limiting step, but since $N = n^f$ and thus $f = \ln N / \ln n$, the number of multiplications required for the kinetic energy is

$$(n/\ln n)N \ln N \cong 4N \ln N, \quad (2.7)$$

for $n = 10$. For $N = 10^6$, (e.g., a four-atom system with $J = 0, f = 6$, with $n = 10$), Eq. (2.7) gives 60×10^6 multiplications (1 s on a 60 megaflop computer) compared to $N^2 = 10^{12}$ multiplications if the \mathbf{H} matrix were full.

It might appear that the direct product grid in Eq. (2.6)

is very limiting. That is, often one likes to choose more complicated coordinates that approximately follow the shape of the potential energy surface and then lay down a grid in these coordinates. While this might in fact produce a more efficient set of points, it is highly system dependent (i.e., not "generic") and much of the benefit of this is actually accomplished by using the energy cut-off procedure discussed in the paragraph before Eq. (2.5). One thus imagines first laying down an infinite three-dimensional grid in x, y , and z for Eq. (2.6), but then proceeds to discard all points (x_i, y_j, z_k) at which the potential energy is larger than some cut-off value V_c ,

$$V(x_i, y_j, z_k) \equiv V_{ijk} > V_c. \quad (2.8)$$

As discussed with regard to Eq. (2.5), this corresponds to setting the wave function to zero at all points that are in classically inaccessible regions for all states with energies $< V_c$. Furthermore, this procedure generates a *nondirect product* grid that is automatically adapted to the shape of the potential energy surface and it can be systematically tested for convergence simply by increasing the energy cutoff V_c .

Finally, we note that it is also possible to use a modified version of this DVR scheme with curvilinear coordinates. For the case of a particle in three dimensions, e.g., the Hamiltonian operator in spherical coordinates (r, θ, ϕ) is

$$H = -\frac{\hbar^2}{2m} \frac{1}{r} \frac{\partial^2}{\partial r^2} r - \frac{\hbar^2}{2mr^2} \left(\frac{\partial^2}{\partial \theta^2} + \cot \theta \frac{\partial}{\partial \theta} \right) - \frac{\hbar^2}{2mr^2 \sin^2 \theta} \frac{\partial^2}{\partial \phi^2} + V(r, \theta, \phi). \quad (2.9)$$

Since the volume element is $dr d\theta d\phi r^2 \sin \theta$ and

$$\frac{\partial^2}{\partial \theta^2} + \cot \theta \frac{\partial}{\partial \theta} = (\sin \theta)^{-1/2} \frac{\partial^2}{\partial \theta^2} (\sin \theta)^{1/2} + \frac{1 + \sin^2 \theta}{4 \sin^2 \theta}, \quad (2.10)$$

a typical matrix element of \mathbf{H} between basis functions has the form

$$\langle \chi_\lambda | H | \chi_\lambda \rangle = \int_0^\infty dr \int_0^\pi d\theta \int_0^{2\pi} d\phi \chi_\lambda \cdot (r\theta\phi) r \sqrt{\sin \theta} \left[-\frac{\hbar^2}{2m} \frac{\partial^2}{\partial r^2} - \frac{\hbar^2}{2mr^2} \frac{\partial^2}{\partial \theta^2} - \frac{\hbar^2}{2mr^2 \sin^2 \theta} \frac{\partial^2}{\partial \phi^2} - \frac{\hbar^2(1 + \sin^2 \theta)}{8mr^2 \sin^2 \theta} + V(r, \theta, \phi) \right] r \sqrt{\sin \theta} \chi_\lambda(r\theta\phi). \quad (2.11)$$

The transformation matrix¹¹ from basis function space to grid point space is thus

$$U_{ijk, \lambda} = \sqrt{\Delta r \Delta \theta \Delta \phi} r_i \sqrt{\sin \theta_j} \chi_\lambda(r_i, \theta_j, \phi_k) \quad (2.12)$$

and the DVR of \mathbf{H} is

$$H_{ijk, i'j'k'} = T_{ii'}^r \delta_{jj'} \delta_{kk'} + T_{jj'}^\theta \frac{\delta_{ii'} \delta_{kk'}}{r_i^2} + T_{kk'}^\phi \frac{\delta_{ii'} \delta_{jj'}}{r_i^2 \sin^2 \theta_j} + \delta_{ii'} \delta_{jj'} \delta_{kk'} \left[V(r_i, \theta_j, \phi_k) - \frac{\hbar^2(1 + \sin^2 \theta_j)}{8mr_i^2 \sin^2 \theta_j} \right]. \quad (2.13)$$

The one-dimensional kinetic energy matrices for the r , θ , and

ϕ degrees of freedom are given in Appendix A [Eqs. (A8), (A9), and (A12)]. Even with non-Cartesian coordinates, therefore, all the important simplicities of a DVR Hamiltonian remain.

III. DVR FOR THE S-MATRIX VERSION OF THE KOHN VARIATIONAL PRINCIPLE

We first summarize the basic formulas of the S -matrix Kohn method^{3(d)} for the case of a collinear $A + BC \rightarrow AB + C$ reaction; from previous work,^{5(a)-5(c)} it is clear how the expressions generalize. The S matrix for the $\gamma n \rightarrow \gamma' n'$ transition ($\gamma =$ arrangement index, $\gamma = a$ for

$A + BC$ and c for $AB + C$, and n is the diatom vibrational state) is

$$\{S_{\gamma'n',\gamma n}\} \equiv \mathbf{S} = \frac{i}{\hbar} (\mathbf{B} - \mathbf{C}^T \cdot \mathbf{B}^* \cdot \mathbf{C}), \quad (3.1a)$$

where matrices $\{B_{\gamma'n',\gamma n}\}$ and $\{C_{\gamma'n',\gamma n}\}$ are given by

$$\mathbf{B} = \mathbf{M}_{00} - \mathbf{M}_0^T \cdot \mathbf{M}^{-1} \cdot \mathbf{M}_0, \quad (3.1b)$$

$$\mathbf{C} = \mathbf{M}_{10} - \mathbf{M}_0^* \cdot \mathbf{M}^{-1} \cdot \mathbf{M}_0. \quad (3.1c)$$

All matrices \mathbf{M} are matrix elements of $(H - E)$, H being the total Hamiltonian and E the total energy. \mathbf{M}_{00} and \mathbf{M}_{10} are "free-free" matrices

$$(\mathbf{M}_{00})_{\gamma'n',\gamma n} = \langle \Phi_{\gamma'n'} | H - E | \Phi_{\gamma n} \rangle, \quad (3.2a)$$

$$(\mathbf{M}_{10})_{\gamma'n',\gamma n} = \langle \Phi_{\gamma'n'}^* | H - E | \Phi_{\gamma n} \rangle, \quad (3.2b)$$

where $\Phi_{\gamma n}(r_\gamma, R_\gamma)$ is a "free" function whose asymptotic ($R_\gamma \rightarrow \infty$) form is

$$\Phi_{\gamma n}(r_\gamma, R_\gamma) \sim \phi_n^\gamma(r_\gamma) e^{-ik_{\gamma n} R_\gamma} v_{\gamma n}^{-1/2}, \quad (3.2c)$$

ϕ_n^γ is the vibrational eigenfunction for state n of arrangement γ and $v_{\gamma n} \equiv \hbar k_{\gamma n} / \mu_\gamma$ is the translational velocity for channel γn . [Note that wave functions in the bra symbol $\langle |$ of \mathbf{M} -matrix elements are *not* complex conjugated unless it is indicated explicitly, e.g., in Eq. (3.2b).] \mathbf{M} is a matrix of $(H - E)$ between an L^2 (square integrable) basis $\{\chi_\lambda(r, R)\}$ that spans the interaction region

$$(\mathbf{M})_{\lambda',\lambda} = \langle \chi_{\lambda'} | H - E | \chi_\lambda \rangle. \quad (3.3)$$

In most work to date,⁵ we have chosen the L^2 basis to be a direct product of channel eigenfunctions $\{\phi_n^\gamma\}$ and a translational basis of distributed Gaussians

$$\chi_\lambda = \phi_n^\gamma(r_\gamma) u_i(R_\gamma), \quad (3.4)$$

so that $\lambda \equiv \gamma n i$, but we have noted several times^{1(b),5(c)} that any L^2 basis that spans the interaction region is suffi-

cient. \mathbf{M}_0 is a rectangular basis of bound-free matrix elements

$$(\mathbf{M}_0)_{\lambda,\gamma n} = \langle \chi_\lambda | H - E | \Phi_{\gamma n} \rangle. \quad (3.5)$$

The essential task in the Kohn calculation is thus to compute the various matrix elements of $(H - E)$ in Eqs. (3.2), (3.3), and (3.5), and then to solve the simultaneous linear equations $\mathbf{M} \cdot \mathbf{X} = \mathbf{M}_0$ to obtain $\mathbf{X} \equiv \mathbf{M}^{-1} \cdot \mathbf{M}_0$.

We now choose the L^2 basis to be a two-dimensional (for this collinear $A + BC$ system) DVR of the type discussed in Sec. II. There is the question of which coordinate system should be used to define the grid and we have made the simplest choice we can imagine, namely a Cartesian grid in the normal modes of the transition state (see Fig. 3). We have in fact learned how to define a DVR in terms of the Jacobi coordinates of both arrangements¹⁸—analogous to the basis sets [Eq. (3.4)] that we have used previously⁵—but the disadvantage of this is that the kinetic energy matrix would then be a full, nonsparse matrix. To retain the advantages of a sparse kinetic energy matrix, therefore, we choose the DVR for the L^2 basis in terms of *one* set of coordinates. (Hyperspherical coordinates are another set that could be used in this way to define the L^2 grid.) Again, our strategy is to lay down the DVR grid in very simple coordinates—so that the kinetic energy matrix will be simple and sparse—and then to adapt the grid to the shape of the specific potential energy surface by discarding points through the energy cut-off criteria of Eq. (2.8).

If $\{x_i\}$ and $\{y_j\}$ denote the grid in the two Cartesian coordinates, then the L^2 matrix \mathbf{M} is

$$\begin{aligned} (\mathbf{M})_{ij,i'j'} &= H_{ij,i'j'} - E \delta_{ii'} \delta_{jj'} \\ &= T_{ii'} \delta_{jj'} + T_{jj'} \delta_{ii'} + \delta_{ii'} \delta_{jj'} [V(x_i, y_j) - E], \end{aligned} \quad (3.6)$$

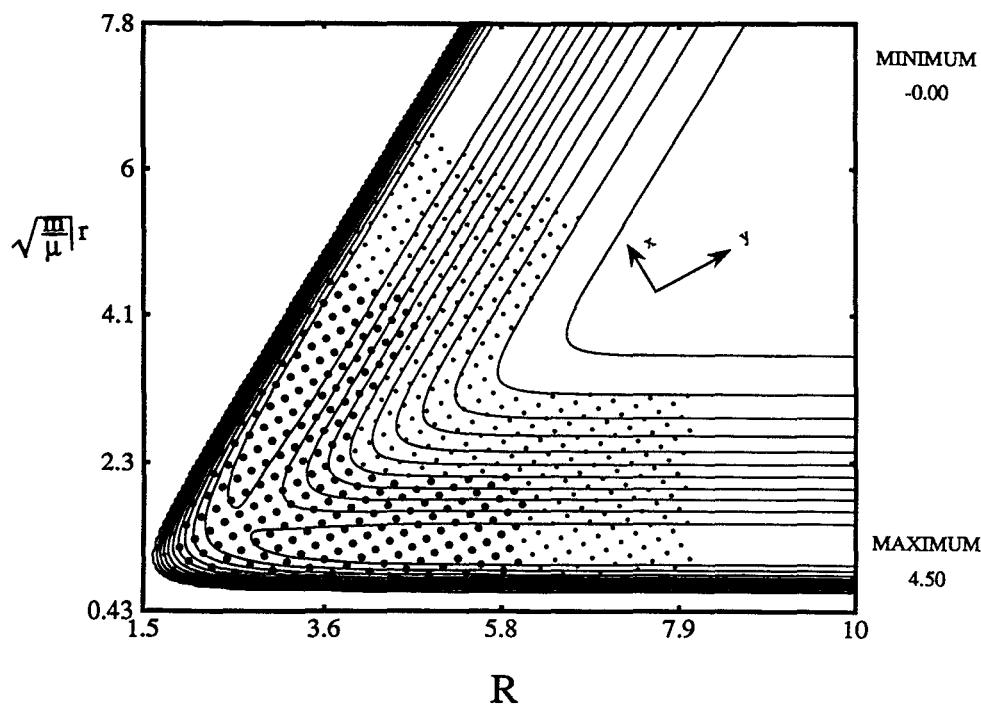


FIG. 3. The contour plot of the LSTH potential energy surface for the $H + H_2 \rightarrow H_2 + H$ reaction in mass-weighted Jacobi coordinates. The points indicate the DVR grid in mass-weighted normal coordinates (x, y) of the transition state. The larger grid (the smaller points, which also line underneath the larger points) results from cut-off parameters $V_c = 4$ eV and $R_{\max} = 8 a_0$ and the smaller grid (the larger points) is the one obtained with $V_c = 2$ eV and $R_{\max} = 6 a_0$.

TABLE II. Converged reaction probabilities for collinear $\text{H} + \text{H}_2(v) \rightarrow \text{H}_2(v') + \text{H}$ at total energy $E = 0.9678$ eV for the LSTH potential surface.

$v-v'$	$P_{v'-v}$
0-0	0.611 53
0-1	0.236 13
1-1	0.422 00

where the two one-dimensional kinetic energy matrices are of the form given by Eq. (2.1). The bound-free matrix \mathbf{M}_0 is

$$(\mathbf{M}_0)_{ij,\gamma n} = \sqrt{\Delta x \Delta y} \langle x_i y_j | H - E | \Phi_{\gamma n} \rangle; \quad (3.7)$$

i.e., one lets $(H - E)$ operate on the free function $\Phi_{\gamma n}(r_\gamma, R_\gamma)$ and then evaluates this at the coordinates (x_i, y_j) . Thus no integrals are required to obtain \mathbf{M} and \mathbf{M}_0 in Eqs. (3.1), but the free-free matrix elements \mathbf{M}_{00} and \mathbf{M}_{10} —matrices that are the size of the number of open channels—are at present still evaluated by separate numerical quadrature.

IV. TEST CALCULATIONS FOR SOME COLLINEAR REACTIONS

A. $\text{H} + \text{H}_2$

An obvious choice for the first test of the DVR S -matrix Kohn methodology described in Sec. III is the collinear $\text{H} + \text{H}_2 \rightarrow \text{H}_2 + \text{H}$ reaction. Figure 3 shows a contour plot of the LSTH potential surface in mass-weighted coordinates. As described in Sec. III, a direct product grid is first laid down in the normal mode coordinates (x, y) of the transition state and the grid is then truncated by the energy cut-off criterion [the two-dimensional version of Eq. (2.8)]. The grid, the L^2 basis of the S -matrix Kohn approach, is also truncated at a value R_{\max} , the translational coordinate in the reactant and product valleys.

Figure 3 shows the grid so obtained for two choices of the parameters V_c and R_{\max} ; the larger grid (denoted by the smaller points) is obtained with $V_c = 4$ eV and $R_{\max} = 8 a_0$ and the smaller grid (denoted by the larger points) with the values $V_c = 2$ eV and $R_{\max} = 6 a_0$. The larger grid gives extremely well-converged results, while the smaller grid is the smallest one which gives the reaction probabilities accurate to a few percent.

The S -matrix Kohn calculation was carried out at a variety of total energies E and the convergence properties were essentially the same at all energies. We thus show the various convergence characteristics for a representative value $E = 0.9678$ eV, for which two vibrational states of H_2 are energetically open channels (in each arrangement). Table II gives the converged reaction probabilities for this energy. Figure 4 shows the relative error in the three reaction probabilities ($0 \rightarrow 0$, $0 \rightarrow 1 = 1 \rightarrow 0$ and $1 \rightarrow 1$) as a function of (a) n_B the number of grid points per de Broglie wavelength; (b) the energy cutoff V_c ; and (c) the asymptotic translational cutoff R_{\max} . n_B the number of grid points per de Broglie wavelength is defined as

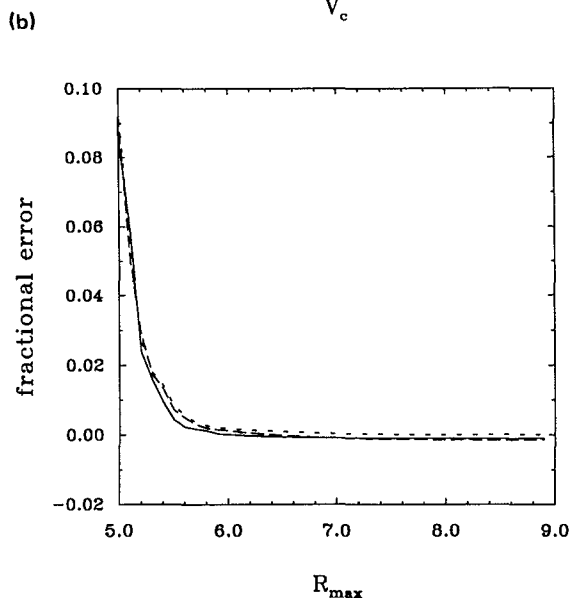
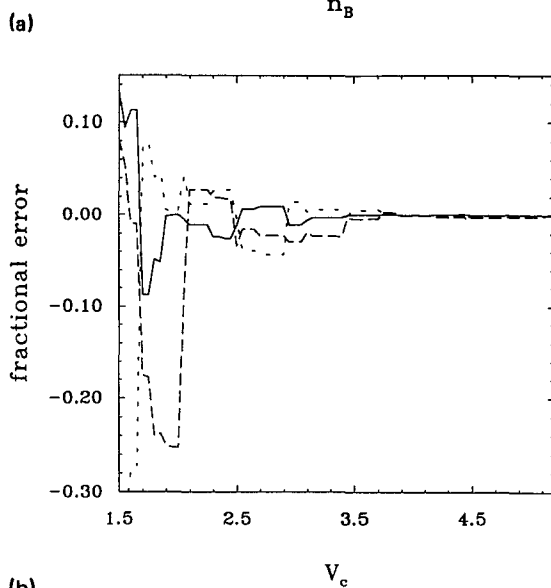
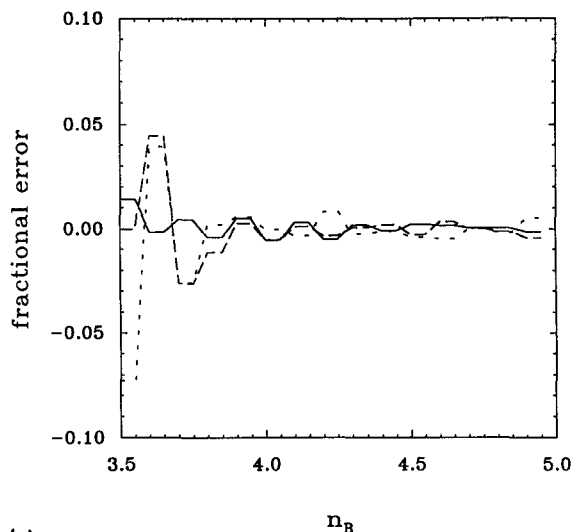


FIG. 4. Convergence of the reaction probabilities (solid line $0 \rightarrow 0$, long dashed line $0 \rightarrow 1$, and short dashed line $1 \rightarrow 1$) for the collinear reaction $\text{H} + \text{H}_2(v) \rightarrow \text{H}_2(v') + \text{H}$ at a typical energy $E = 0.9678$ eV as a function of (a) n_B the number of grid points per de Broglie wavelength [Eq. (4.1)]; (b) the energy cutoff V_c ; and (c) the channel radius cutoff R_{\max} .

$$n_B = 2\pi/(k_x \Delta x) \equiv 2\pi/(k_y \Delta y), \quad (4.1)$$

where $k_x = \sqrt{2m_x E/\hbar^2}$ and $k_y = \sqrt{2m_y E/\hbar^2}$; i.e., Δx and Δy are chosen to be the same in mass-weighted coordinates.

Figure 4 shows that convergence to a relative accuracy of $\sim 1\%$ is achieved with $n_B \cong 3.8$, $V_c \cong 3.5$ eV, and $R_{\max} \cong 5.5 a_0$. This corresponds to a total of 221 grid points, which is only $\sim 15\%$ more than the number of conventional basis functions (e.g., ~ 24 translational functions \times four vibrational functions \times two arrangements = 192) needed to achieve this level of convergence. This is clearly an extremely encouraging result, namely that the number of grid points required is not much larger than the number of basis functions. Were this to be true in general, the DVR procedure would clearly be the preferable way to go because it eliminates integral evaluation and because the DVR Hamiltonian matrix is so sparse and simple to construct.

For this simple test, the free wave functions [Eq. (3.2)] were an undistorted incoming wave $\exp(-ikR)$ (multiplied^{3(d)} by a smooth cut-off function to regularize it at $R \rightarrow 0$), but it has been noted before^{5(c)} that the L^2 basis can be reduced by using *distorted* free waves. Within the present methodology, this would allow one to use a smaller value of the parameter R_{\max} , thus reducing the size of the DVR grid for the L^2 space. This will clearly be a useful thing to do for challenging applications.

B. Cl + HCl

Heavy + light-heavy reactions have very unusual dynamical features because of the mass disparities. Specifically, the dynamics tends to violate the assumptions of transition state theory quite strongly because the H atom hops back and forth between the Cl atoms several times during a reactive collision. It is thus of interest to see how well the present DVR version of the S -matrix Kohn method can describe this kind of dynamics.

We thus consider the prototype of this class of reactions $\text{Cl} + \text{HCl} \rightarrow \text{ClH} + \text{Cl}$ using the same LEPS potential energy surface as Bondi *et al.*¹⁹ in their quantum, semiclassical, and classical studies. Figure 5 shows the potential energy surface for the $\text{Cl} + \text{HCl}$ reaction in mass-weighted coordinates with a typical DVR grid superimposed on it. Results given by the present DVR S -matrix Kohn calculation are shown in Fig. 6 for the $0 \rightarrow 0$ reaction probability as a function of energy, up to a value slightly above the $v = 1$ channel of HCl. Agreement with the results of Bondi *et al.* is excellent.

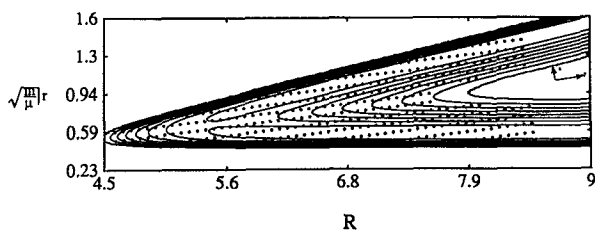


FIG. 5. The contour plot of the LEPS potential energy surface of Ref. 19 for the $\text{Cl} + \text{HCl} \rightarrow \text{ClH} + \text{Cl}$ reaction in mass-weighted Jacobi coordinates. The points indicate a typical DVR grid.

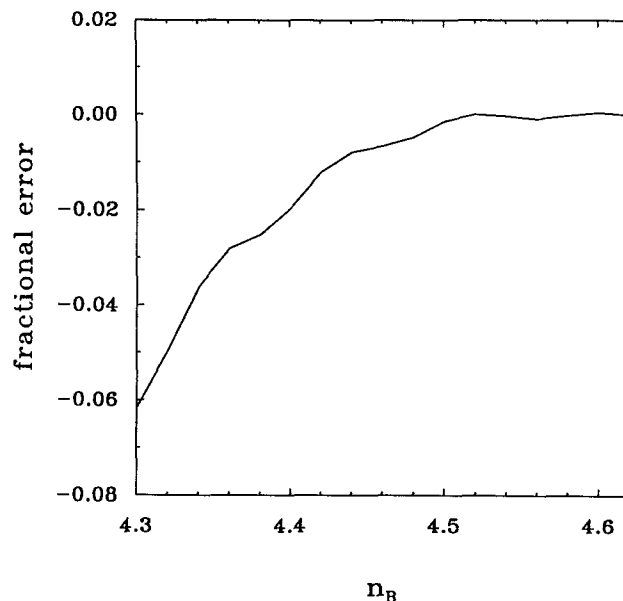


FIG. 7. Convergence of the $0 \rightarrow 0$ and reaction probability for the $\text{Cl} + \text{HCl} \rightarrow \text{ClH} + \text{Cl}$ reaction at energy $E = 0.375$ eV as a function of n_B the number of grid points per de Broglie wavelength [as in Fig. 4(a) for the $\text{H} + \text{H}_2$ reaction].

Figure 7 shows the convergence of the $0 \rightarrow 0$ reaction probability at total energy $E = 0.375$ eV as a function of the number of grid points per de Broglie wavelength, i.e., n_B of Eq. (4.1). As for the $\text{H} + \text{H}_2$ reaction [cf., Fig. 4(a)], one sees that convergence is achieved with $n_B \cong 4.5$. It is very encouraging to see that convergence with respect to this “dimensionless grid spacing” is approximately the same for the very disparate examples treated in the paper.

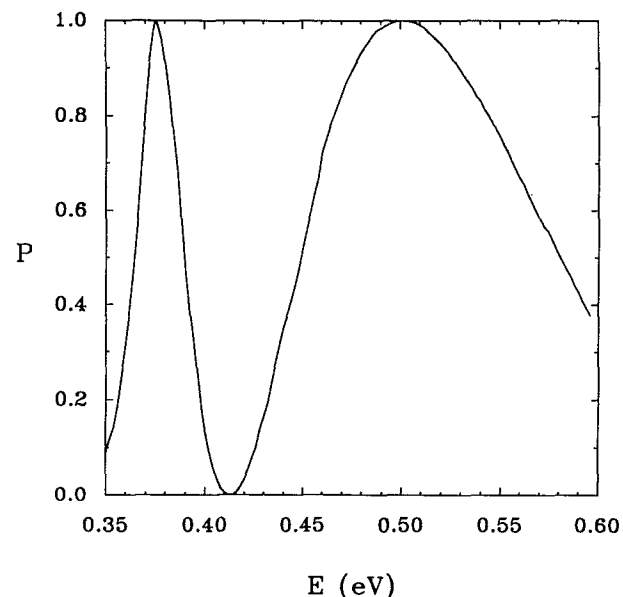


FIG. 6. Reaction probability calculated for the $\text{Cl} + \text{HCl}(v = 0) \rightarrow \text{ClH}(v' = 0) + \text{Cl}$ collinear reaction as a function of energy E .

V. CONCLUDING REMARKS

The primary purpose of this paper has been to show that a set of grid points, i.e., a discrete variable representation (DVR), provides a very efficient and easy-to-use L^2 basis for the S -matrix version of the Kohn method for quantum reactive scattering. This is the first DVR scheme that has proved practical for reactive scattering calculations. An important conclusion from these test calculations is that the number of grid points required for a comparable degree of convergence is only 10%–20% more than the number of conventional basis functions (e.g., channel eigenfunctions \times distributed Gaussians) used in previous S -matrix Kohn calculations.^{5(a)–5(c)} This is extremely encouraging with regard to the possibility of carrying out such calculations for more complex systems because a DVR avoids integral evaluation in order to obtain the Hamiltonian matrix and also because the Hamiltonian matrix is extremely sparse.¹¹ Quasiadiabatic,^{9(a),9(b)} or other contraction schemes used with conventional basis functions can also be employed in an identical fashion with this DVR.

The particular DVR we have devised is extremely simple and has a universal character. The Hamiltonian matrix, and all aspects of the calculations, involve only the grid points themselves with no explicit reference to an underlying basis from which the DVR comes. It is clear that this particular DVR can also be used readily for eigenvalue problems as well as the present S -matrix Kohn scattering calculations.

For both applications in Sec. IV, the DVR was laid down in the rectilinear normal coordinates of the transition state. It is perhaps not surprising that this set of coordinates works well for the Cl + HCl reaction because for this heavy + light-heavy case, these coordinates are very close to the reactant and product Jacobi coordinates (and also to hyperspherical coordinates). It was not so obvious that these coordinates would work so well for H + H₂ because they differ substantially from the reactant and product coordinates in the asymptotic regions (see Fig. 3). It is gratifying to see that in fact they do work quite well also for the H + H₂ reaction. This supports our current thinking that it really does not matter much which coordinates one uses to lay down the grid, provided that it covers the space; the energy cut-off criterion [e.g., Eq. (2.8)] then adapts the grid to the shape of the potential energy surface for the specific system being treated. This will be particularly important for complex systems, where it would be very difficult to guess the “best” coordinate system intuitively. The conclusion from the present work is that one puts the grid down in the simplest coordinates possible—so that the kinetic energy matrix is simple and sparse—and the energy cut-off criterion then adapts it to the shape of the given potential energy surface.

The convergence tests for both the harmonic oscillator of Sec. II B and the two reactions in Sec. IV all suggest that reasonable accuracy is obtained with \sim four to five grid points per de Broglie wavelength. This thus provides a universal rule of thumb for estimating the grid spacing, the primary parameter that specifies this DVR.

Further applications are of course necessary to see if all of these potential advantages will in fact be realized.

APPENDIX A: A SIMPLE GENERIC DVR

Consider a one-dimensional quantum system with coordinate x restricted to the interval (a, b) . The kinetic energy operator is

$$T = -\frac{\hbar^2}{2m} \frac{d^2}{dx^2} \quad (\text{A1})$$

and we consider first the case that the wave functions vanish at the endpoints a and b . The grid $\{x_i\}$ for the DVR is equally spaced

$$x_i = a + (b - a)i/N, \quad i = 1, \dots, N - 1 \quad (\text{A2})$$

and the associated functions for a uniform grid are Fourier functions (i.e., particle-in-a-box eigenfunctions)

$$\phi_n(x) = \left(\frac{2}{b-a}\right)^{1/2} \sin\left[\frac{n\pi(x-a)}{b-a}\right], \quad n = 1, \dots, N - 1. \quad (\text{A3})$$

Note that $\phi_n(x_0 \equiv a) = \phi_n(x_N \equiv b) = 0$; there are thus $N - 1$ functions and $N - 1$ points.

The DVR, or grid point representation of the kinetic energy is then given by

$$T_{ii'} = -\frac{\hbar^2}{2m} \Delta x \sum_{n=1}^{N-1} \phi_n(x_i) \phi_n''(x_{i'}), \quad (\text{A4})$$

where $\Delta x = (b - a)/N$ is the grid spacing. With the above definitions, this becomes

$$T_{ii'} = \frac{\hbar^2}{2m} \left(\frac{\pi}{b-a}\right)^2 \frac{2}{N} \sum_{n=1}^{N-1} n^2 \sin\left(\frac{n\pi i}{N}\right) \sin\left(\frac{n\pi i'}{N}\right). \quad (\text{A5})$$

The calculation is tedious, but the sum over n can be evaluated analytically.²⁰ One obtains

$$T_{ii'} = \frac{\hbar^2}{2m} \frac{(-1)^{i-i'}}{(b-a)^2} \frac{\pi^2}{2} \left\{ \frac{1}{\sin^2[\pi(i-i')/2N]} - \frac{1}{\sin^2[\pi(i+i')/2N]} \right\} \quad (\text{A6a})$$

for $i \neq i'$ and

$$T_{ii} = \frac{\hbar^2}{2m} \frac{1}{(b-a)^2} \frac{\pi^2}{2} \left[(2N^2 + 1)/3 - \frac{1}{\sin^2(\pi i/N)} \right]. \quad (\text{A6b})$$

We now consider several specific cases.

1. $(-\infty, \infty)$ interval

In this case, $a \rightarrow -\infty$, $b \rightarrow \infty$, so a finite grid spacing $\Delta x = (b - a)/N$ requires that $N \rightarrow \infty$ also. With $\{x_i\}$ defined as in Eq. (A2), one also has $i + i' \rightarrow \infty$, but $i - i'$ is finite. Equation (A6) thus becomes

$$T_{ii'} = \frac{\hbar^2}{2m\Delta x^2} (-1)^{i-i'} \left\{ \frac{\pi^2/3}{(i-i')^2}, \quad i \neq i' \right\}, \quad (\text{A7})$$

and the grid is now specified more conveniently as $x_i = i\Delta x$, $i = 0, \pm 1, \pm 2, \dots$.

2. $(0, \infty)$ interval

This is appropriate for a radial coordinate r . In this case, $a = 0$, $b \rightarrow \infty$ and also $N \rightarrow \infty$, so that the grid spacing

$\Delta r = (b - a)/N$ is finite. In this case, both $i + i'$ and $i - i'$ are finite and Eq. (A6) becomes

$$T_{ii'} = \frac{\hbar^2}{2m\Delta r^2} (-1)^{i-i'} \left\{ \begin{array}{ll} \frac{\pi^2/3 - 1/2i^2}{2} & i = i' \\ \frac{2}{(i-i')^2} - \frac{2}{(i+i')^2} & i \neq i' \end{array} \right\}, \quad (\text{A8})$$

with

$$r_i = i\Delta r, \quad i = 1, \dots$$

Note that the matrix element vanishes if i or $i' = 0$, i.e., the origin $r = 0$ itself is not a point in the grid.

3. $(0, \pi)$ interval

This is the case of a polar coordinate θ , for which the functions also vanish at the endpoints. In this case, N is finite for a finite grid spacing. Since $a = 0$ and $b = \pi$, Eq. (A6) reads

$$T_{ii'} = \frac{\hbar^2}{2m} \frac{(-1)^{i-i'}}{2} \left\{ \frac{1}{\sin^2[\pi(i-i')/2N]} - \frac{1}{\sin^2[\pi(i+i')/2N]} \right\} \quad (\text{A9a})$$

for $i \neq i'$, and

$$T_{ii} = \frac{\hbar^2}{2m} \frac{1}{2} \left[(2N^2 + 1)/3 - \frac{1}{\sin^2(\pi i/N)} \right], \quad (\text{A9b})$$

with

$$\theta_i = i\pi/N, \quad i = 1, \dots, N-1.$$

Here the matrix element vanishes if i or $i' = 0$ or N ; i.e., the points $\theta = 0$ and π are not points in the grid.

4. $(0, 2\pi)$ interval

This is the case of an azimuthal coordinate ϕ and the boundary conditions in this case are that the wave function is periodic. This case has been treated by Meyer²¹ some time ago, but for completeness we show briefly how the present methodology applies to it. The appropriate basis functions are

$$\Phi_n(\phi) = \frac{e^{in\phi}}{\sqrt{2\pi}}, \quad n = 0, \pm 1, \pm 2, \dots, \pm N \quad (\text{A10a})$$

and the $2N + 1$ distinct grid points are

$$\phi_i = i \frac{2\pi}{2N+1}, \quad i = 1, \dots, 2N+1. \quad (\text{A10b})$$

The matrix of the kinetic energy operator in the DVR is thus

$$T_{ii'} = \frac{\hbar^2}{2m} \Delta\phi \sum_{n=-N}^N n^2 \frac{e^{in(\phi_i - \phi_{i'})}}{2\pi} \quad (\text{A11})$$

and a calculation similar to that above gives

$$T_{ii'} = \frac{\hbar^2}{2m} (-1)^{i-i'} \times \left\{ \begin{array}{ll} \frac{N(N+1)}{3}, & i = i' \\ \frac{\cos[\pi(i-i')/2N+1]}{2 \sin^2[\pi(i-i')/2N+1]}, & i \neq i' \end{array} \right\}, \quad (\text{A12})$$

which is the same as that given by Meyer.²¹

Finally, we note that even though we have emphasized in the paper that Eq. (A7), e.g., has a universal character, being independent of my specific underlying set of basis functions, it is nevertheless possible to determine what set of basis functions corresponds to this infinite uniform grid. Thus, if $|x_i\rangle$ is the Dirac state for grid point i of the DVR [cf. Eq. (A2)], then the wave function for this state is

$$\langle x|x_i\rangle = \sum_{n=1}^{N-1} \phi_n(x) \phi_n(x_i) \quad (\text{A13})$$

for the finite Fourier expansion of Eqs. (A2)–(A3), or more specifically,

$$\langle x|x_i\rangle = \frac{2}{b-a} \sum_{n=1}^{N-1} \sin\left[\frac{n\pi(x-a)}{b-a}\right] \sin\left[\frac{n\pi(x_i-a)}{b-a}\right]. \quad (\text{A14})$$

This sum can, as before, be evaluated analytically, and when one takes the limit $(b-a) \rightarrow \infty$, $N \rightarrow \infty$, $(b-a)/N = \Delta x$, the result is

$$\langle x|x_i\rangle = \sin[\pi(x-x_i)/\Delta x] / [\pi(x-x_i)]. \quad (\text{A15})$$

This wave function has the properties that it is $1/\Delta x$ for $x = x_i$ and zero for $x = x_{i'}$, $i' \neq i$ and has the limit $\delta(x-x_i)$ as $\Delta x \rightarrow 0$. Furthermore, precisely this same result [Eq. (A15)] is obtained from the infinite order Lagrangian interpolation polynomials utilized in Appendix B. That is Eq. (A15) does not rely on the fact that we utilized a finite Fourier basis and then took the infinite limit in order to derive it; it is a general result independent of the basis used. Equation (A15) thus makes it possible to have a complete wave function from a DVR calculation, so that one can obtain values of the wave function at coordinates other than at the DVR grid points.

APPENDIX B: INFINITE ORDER FINITE DIFFERENCE

The $(2N+1)$ -order Lagrangian interpolation formula for a function $f(x)$ is²²

$$f(x) = \sum_{k=-N}^N f_k \prod_{l=-N}^N \prime \left(\frac{x-x_l}{x_k-x_l} \right), \quad (\text{B1})$$

where $f_k = f(x_k)$ and where the prime on the product means that the factor $l = k$ is omitted. We consider the case of equally spaced grid points

$$x_k = k\Delta x, \quad k = 0, \pm 1, \dots, \pm N, \quad (\text{B2})$$

and wish to evaluate the second derivative of $f(x)$ at the central grid point $x_0 = 0$, i.e., $f''(0)$.

Differentiating Eq. (B1) twice and setting $x = 0$ [and utilizing the fact that the grid points are given by Eq. (B4)] gives

$$f''(0) = -\frac{1}{\Delta x^2} \left[2f_0 \sum_{l=1}^N \frac{1}{l^2} - \sum_{k=1}^N (f_k + f_{-k}) \frac{1}{k^2} \times \prod_{l=1}^N \prime \left(\frac{l^2}{l^2 - k^2} \right) \right]. \quad (\text{B3})$$

$N = 1$ and 2 , e.g., give the three- and five-point results, respectively,

$$f''(0) \cong -\frac{1}{\Delta x^2} [2f_0 - (f_1 + f_{-1})]$$

and

$$f''(0) \cong -\frac{1}{\Delta x^2} \left[\frac{5}{2}f_0 - \frac{4}{3}(f_1 + f_{-1}) + \frac{1}{12}(f_2 + f_{-2}) \right].$$

In the limit $N \rightarrow \infty$, one has

$$\lim_{N \rightarrow \infty} \sum_{l=1}^N \frac{1}{l^2} = \sum_{l=1}^{\infty} \frac{1}{l^2} = \frac{\pi^2}{6}, \quad (\text{B4a})$$

$$\begin{aligned} \lim_{N \rightarrow \infty} \prod_{l=1}^N \frac{l^2}{l^2 - k^2} &= \lim_{x \rightarrow k} \left(1 - \frac{x^2}{k^2} \right) \frac{\pi x}{\sin \pi x} \\ &= -2(-1)^k, \end{aligned} \quad (\text{B4b})$$

so that the infinite order result is

$$f''(0) = -\frac{1}{\Delta x^2} \left[f_0 \pi^2/3 + \sum_{k=1}^{\infty} (f_k + f_{-k}) \frac{2(-1)^k}{k^2} \right]. \quad (\text{B5})$$

The coefficients in Eq. (B5) are compared in Table I with several low order finite difference coefficients to indicate the nature of the convergence to the infinite order limit.

ACKNOWLEDGMENTS

We wish to thank Dr. Gerrit Groenenboom for many useful discussions and stimulating interactions regarding this work and also helping prepare Figs. 3 and 5, and also to Professor John Zhang for providing us with the results of "conventional" S -matrix Kohn scattering calculations for the collinear $\text{H} + \text{H}_2$ reaction with which to calibrate our early DVR calculations. W.H.M. also thanks Professor Ronnie Kosloff, Professor Richard Friesner, Professor John Light, and Professor Robert Wyatt for many interesting discussions over the last several years about grid methods in quantum mechanics. This work has been supported by the National Science Foundation, Grant No. CHE-8920690.

¹ For recent reviews, (a) D. E. Manolopoulos and D. C. Clary, *Annu. Rep. C (R. Soc. Chem.)* **86**, 95 (1989); (b) W. H. Miller, *Annu. Rev. Phys. Chem.* **41**, 245 (1990).

² Also see the following papers and references to earlier work of the respective authors therein: (a) M. Zhao, D. G. Truhlar, D. W. Schwenke, C. H. Yu, and D. J. Kouri, *J. Phys. Chem.* **94**, 7062 (1990); (b) J. M. Launay, *Theor. Chem. Acta* **79**, 183 (1991); (c) D. E. Manolopoulos, R. E. Wyatt, and D. C. Clary, *J. Chem. Soc. Faraday Trans.* **86**, 1641 (1990); (d) Y. S. Wu, S. A. Cuccaro, P. G. Hipes, and A. Kuppermann, *Chem. Phys. Lett.* **168**, 429 (1990); (e) G. C. Schatz, *J. Chem. Soc. Faraday Trans.* **86**, 1729 (1990).

³ (a) W. Kohn, *Phys. Rev.* **74**, 1763 (1948); (b) M. Kamimura, *Prog. Theor. Phys. Suppl.* **62**, 236 (1977); (c) W. H. Miller and B. M. D. D. Jansen op de Haar, *J. Chem. Phys.* **86**, 6213 (1987); (d) J. Z. H. Zhang, S.-I. Chu, and W. H. Miller, *ibid.* **88**, 6233 (1988).

⁴ (a) C. Schwartz, *Phys. Rev.* **124**, 1468 (1961); *Ann. Phys.* **10**, 36 (1961); (b) R. K. Nesbit, *Variational Methods in Electron-Atom Scattering Theory* (Plenum, New York, 1980), pp. 30–50.

⁵ (a) J. Z. H. Zhang and W. H. Miller, *Chem. Phys. Lett.* **153**, 465 (1988); (b) **159**, 130 (1989); (c) *J. Chem. Phys.* **91**, 1528 (1989); (d) D. E. Manolopoulos and R. E. Wyatt, *Chem. Phys. Lett.* **159**, 123 (1989); (e) *J. Chem. Phys.* **91**, 6096 (1989); (f) M. D'Mello, D. E. Manolopoulos, and R. E. Wyatt, *ibid.* **94**, 5985 (1991); (g) J. M. Launay and M. LeDourneuf, *Chem. Phys. Lett.* **163**, 178 (1989); (h) M. Zhao, D. G. Truhlar, D. W. Schwenke, and D. J. Kouri, *J. Phys. Chem.* **94**, 7074 (1990); (i) N. C. Blais, M. Zhao, D. G. Truhlar, D. W. Schwenke, and D. J. Kouri, *Chem. Phys. Lett.* **166**, 11 (1990).

⁶ J. Z. H. Zhang, *Chem. Phys. Lett.* **181**, 63 (1991).

⁷ (a) K. Haug, D. W. Schwenke, D. G. Truhlar, Y. Zhang, Z. H. Zhang, and D. J. Kouri, *J. Chem. Phys.* **87**, 1892 (1987); (b) J. Z. H. Zhang, D. J. Kouri, K. Haug, D. W. Schwenke, Y. Shima, and D. G. Truhlar, *ibid.* **88**, 2492 (1988); (c) H. Koizumi and G. C. Schatz, in *Molecular Vibrations*, edited by J. M. Bowman and M. Ratner (JAI, Greenwich, CT, 1991); (d) Y. C. Zhang, J. Z. H. Zhang, D. J. Kouri, K. Haug, D. W. Schwenke, and D. G. Truhlar, *Phys. Rev. Lett.* **60**, 2367 (1988).

⁸ (a) T. N. Rescigno, C. W. McCurdy, and B. I. Schneider, *Phys. Rev. Lett.* **63**, 248 (1989); (b) T. N. Rescigno, B. H. Lengsfeld III, and C. W. McCurdy, *Phys. Rev. A* **41**, 2462 (1990); (c) B. I. Schneider, T. N. Rescigno, and C. W. McCurdy, *ibid.* **42**, 3132 (1990); (d) B. I. Schneider, T. N. Rescigno, B. H. Lengsfeld III, and C. W. McCurdy, *Phys. Rev. Lett.* **66**, 2728 (1991).

⁹ (a) Z. Bacic and J. C. Light, *J. Chem. Phys.* **85**, 4594 (1986); **86**, 3065 (1987); (b) J. Z. H. Zhang and W. H. Miller, *J. Phys. Chem.* **94**, 7785 (1990); (c) D. E. Manolopoulos, M. D'Mello, and R. E. Wyatt, *J. Chem. Phys.* **93**, 403 (1990); (d) M. Zhao, D. G. Truhlar, D. W. Schwenke, C. H. Yu, and D. J. Kouri, *J. Phys. Chem.* **94**, 7062 (1990).

¹⁰ For example, (a) J. M. Bowman, *J. Phys. Chem.* **95**, 4960 (1991); (b) D. C. Clary, *J. Chem. Phys.* **95**, 7298 (1991).

¹¹ (a) J. V. Lill, G. A. Parker, and J. C. Light, *Chem. Phys. Lett.* **89**, 483 (1982); (b) J. C. Light, I. P. Hamiltonian, and J. V. Lill, *J. Chem. Phys.* **82**, 1400 (1985); (c) J. V. Lill, G. A. Parker, and J. C. Light, *ibid.* **85**, 900 (1986); (d) S. E. Choi and J. C. Light, *ibid.* **92**, 2129 (1990); (e) J. C. Light, R. M. Whitnell, T. J. Park, and S. E. Choi, *NATO ASI Ser. C* **277**, 187 (1989).

¹² (a) D. O. Harris, G. G. Engerholm, and W. D. Gwinn, *J. Chem. Phys.* **43**, 1515 (1965); (b) P. F. Endres, *ibid.* **47**, 798 (1967); (c) A. S. Dickinson and P. R. Certain, *J. Chem. Phys.* **49**, 4209 (1968).

¹³ (a) W. Yang and A. C. Peet, *Chem. Phys. Lett.* **153**, 98 (1988); (b) A. C. Peet and W. Yang, *J. Chem. Phys.* **90**, 1746 (1989); (c) **92**, 522 (1990).

¹⁴ (a) R. A. Friesner, *Chem. Phys. Lett.* **116**, 39 (1985); (b) *J. Chem. Phys.* **85**, 1462 (1986); (c) **86**, 3522 (1987); (d) Y. Won, J. G. Lee, M. N. Ringnalda, and R. A. Friesner, *ibid.* **94**, 8152 (1991).

¹⁵ (a) C. J. Lanczos, *J. Res. Natl. Bur. Stand.* **45**, 255 (1950); (b) G. C. Groenenboom and H. M. Buck, *J. Chem. Phys.* **92**, 4374 (1990).

¹⁶ (a) A. C. Peet and W. H. Miller, *Chem. Phys. Lett.* **149**, 257 (1988); (b) W. Yang, A. C. Peet, and W. H. Miller, *J. Chem. Phys.* **91**, 7537 (1989).

¹⁷ (a) R. Kosloff, *J. Phys. Chem.* **92**, 2087 (1988), and references to earlier work therein; (b) C. Leforestier, R. H. Bisseling, C. Cerjan, M. O. Feit, R. Friesner, A. Guldberg, A. Hammerich, G. Jolicard, W. Karrlein, H. D. Meyer, N. Lipkin, O. Roncero, and R. Kosloff, *J. Comp. Phys.* **94**, 59 (1991).

¹⁸ D. T. Colbert and W. H. Miller (unpublished work).

¹⁹ (a) D. K. Bondi, J. N. L. Connor, J. Manz, and J. Romelt, *Mol. Phys.* **50**, 467 (1983); (b) D. K. Bondi, J. N. L. Connor, B. C. Garret, and D. G. Truhlar, *J. Chem. Phys.* **78**, 5981 (1983).

²⁰ The product of sines gives $1/2 \cos(nA) - 1/2 \cos(nB)$ with $A = \pi(i - i')/N$ and $B = \pi(i + i')/N$ and then $\sum_{n=1}^{N-1} n^2 \cos(nA) = -(\partial^2/\partial A^2) \text{Re} \sum_{n=1}^{N-1} e^{inA}$ and similarly for the B term. The latter sum is a geometric series, which gives $\text{Re} \sum_{n=1}^{N-1} e^{inA} = -1/2 + 1/2 \sin[(N - 1/2)A]/\sin(A/2)$ and it is then clear how the calculation proceeds.

²¹ R. Meyer, *J. Chem. Phys.* **52**, 2053 (1970).

²² M. Abramowitz and I. A. Stegun, *Handbook of Mathematical Functions* (U.S. Government Printing Office, Washington, D.C., 1964) Number 25.2.2, p. 878.